

Molengraaffsingel 8 2629 JD DELFT The Netherlands

www.tno.nl

T +31 15 820 09 20

## **TNO** report

## TNO 2022 R12801A

Cement recycling with help of biobased materials.

D1.2 Characterization of two types of ultrafine Construction and Demolition Waste Concrete

Date 22 maart 2023

Author(s) Jeanette Visser (TNO)

Juan Garzon-Amortegui (TNO) Sacha Hermanns (TNO)

Ingrid Haaksman, Nicole Engelen, Ted Slaghek, Richard Gosselink

(WFBR)

Virginie Wiktor (Cugla)

Copy no No. of copies

Number of pages 26 (incl. appendices)

Number of appendices Sponsor

Project name Cement recycling with biopolymers

Project number 060.51606/01.01

#### All rights reserved.

No part of this publication may be reproduced and/or published by print, photoprint, microfilm or any other means without the previous written consent of TNO.

In case this report was drafted on instructions, the rights and obligations of contracting parties are subject to either the General Terms and Conditions for commissions to TNO, or the relevant agreement concluded between the contracting parties. Submitting the report for inspection to parties who have a direct interest is permitted.

© 2022 TNO

# Contents

1	Introduction	3
1.1	Background of the project	3
1.2	Aim of this report	3
1.3	Contents of this report	4
2	Materials	5
3	Characterization tests	6
3.1	Solid density	6
3.2	Particle size	6
3.3	Specific surface area	7
3.4	Thermal Gravimetric Analysis	8
3.5	Water demand	g
3.6	Zetapotential	9
3.7	XRF/XRD	-
3.8	TOC (Total Organic Carbon)	11
3.9	Hardening of the pure materials	11
4	Characteristics of the ultrafines	13
4.1	Solid density	13
4.2	Particle size distribution	13
4.3	Specific surface area and porosity	15
4.4	Moisture content	15
4.5	TGA and loss on Ignition	16
4.6	Water demand in the quick consistency test	
4.7	Characteristics of the ultrafines in water	
4.8	XRF	
4.9	XRD	19
4.10	TOC	22
4.11	Hardening of the pure materials	22
5	Discussion and conclusions	24
5.1	Composition	24
5.2	Physical characteristics and water demand	24
5.3	Reactivity	25
6	Signature	26

## 1 Introduction

## **1.1** Background of the project

The currently most used construction material is concrete. This concrete consists mostly of gravel, sand and cement. The cement in the concrete is produced from, amongst others, clay, lime stone and sand, heated in an oven at temperature of ca. 1450 °C. The process produces quite some CO<sub>2</sub>, from the calcination of the raw materials like carbonates but also by the heating process. Globally, the cement production is responsible for 7 % of the CO<sub>2</sub> production annually. The Dutch government wants to reduce the amount of CO<sub>2</sub> produced annually (reaching at least a 50% reduction by 2030 for the construction industry).

At the same time, more and more concrete structures are taken out of service. The old concrete that thus becomes available is recycled as much as possible. The recycling of concrete focusses on the reclamation of sand and aggregates. Its side effect, however, is that larger quantities of old cement paste becomes available, that has to be reused in turn to fulfill also the goals set by the Dutch government for circularity. Old cement paste can be recycled by grinding it to ultra-small particles and use it as filler for new concrete or asphalt. Preferentially, however, it should be re-used as new cement, to fulfill both ambition of the reducing the GHG and increase circularity. This means the old cement paste has to be reactivated. One such reactivation strategy is by re-calcinating the milled old hydrated cement at high temperature. The thermomechanical method still requires quite some energy (which produces also CO<sub>2</sub>) and the results seem not always be beneficial (Kalinowska-Wichrowska, Pawluczuk and Bołtryk, 2020)1. In addition, using old cement in the new cement production was found to lead to a low quality cement (EU project C2CA: 'Cement and aggregates from EOL concrete). Another route at reactivating old cement paste is by chemical activation. The principle process of this chemical reactivation consists of two-step process: dissolving the old cement paste and precipitating its compound in a new, strong, chemical product that will not dissolve in water and have the same performance of the current used cement. This research focuses on this second route, using biobased additives to stimulate the process of dissolution and precipitation. It thus aims at recycling cement via chemical routes, at room temperature and using an alkaline environment in combination with biobased additives.

## **1.2** Aim of this report

In order to be able to select the right biobased materials and to optimize their effect on the activation of the recycled cement, the recycled cements need to characterized. For instance: the (specific) surface of the recycled cement will give an indication of the amount of reactive surface, and the dosage of the biobased material will likely be correlated to that. In addition, to understand possible differences in reactions between different recycled cement types, it is important to quantify their differences.

Although it is not possible a-priori to know which materials' properties of the recycled cements will be of importance in this research, it is possible on the basis of

<sup>&</sup>lt;sup>1</sup> Kalinowska-Wichrowska, K., Pawluczuk, E. and Bołtryk, M. (2020) 'Waste-free technology for recycling concrete rubble', *Construction and Building Materials*. r, 234, p. 117407. doi: 10.1016/j.conbuildmat.2019.117407.

experience and background knowledge to define the properties that are likely of importance, namely:

- Chemical and mineralogical composition.
- Density, particle size distribution and specific surface area.
- Moisture content.
- Dissolution behavior and surface charge characteristics.
- Hardening characteristics on pure materials.

In this report, the results of the characterization of two ultrafine waste streams will be presented. The experiments have been executed by TNO, Cugla and WFBR.

## **1.3** Contents of this report

In Chapter 2, a brief description of the ultrafine materials in the research has been given while in Chapter 3 the test methods are described. Chapter 4 gives the results of the experiments. Chapter 5, finally, gives a brief discussion of the determined characteristics of the ultrafine streams as well as their differences.

## 2 Materials

Two waste streams of ultrafine materials have been delivered by Urban Mine to TNO. The first waste stream arrived on May 18th, 2022 in a big bag. After arrival, 13 samples have been taken randomly and stored in air-tight buckets. The remaining material in the big bag has been wrapped in cling foil and stored to prevent ageing due to moisture ingress. The buckets have been coded at TNO as MP2017, with sub-numbers 01 to 13. From each bucket buckets, one or more subsamples have been taken randomly and tested for solid density and particle size distribution, as quality check of the sampling. After validation of the homogeneity, bucket MP2017-13 has been delivered to WFBR and bucket MP2017-06 to Cugla. The remaining buckets have been stored at TNO and used for testing.

On 17 October 2022, 10 buckets have been received from Urban Mine with CCDW from sleepers. Tw buckets have been sent to WFBR, the other 8 have been stored at TNO and used for testing. At TNO, the buckets have been given sample number MP2035, subcoding 1-8.

According to the information of Urban Mine, the process of selecting and recycling the concrete is as follows (email A. Alberda, Dec 21, 2022):

- (1) The first series consists of mixed materials from so-called 'infra-debris', consisting of concrete goods like (sidewalk) tiles and curbs. The products are fed to a so-called precrusher and are next further fragmented in a second crusher, resulting in a sand and a gravel sized stream. Next, the sand fraction goes into a so-called smart refiner, after which three particle fractions are produced: 0.25 4 mm, 0.065-0.25 mm and 0-0.065 mm. The smallest size has been sent for investigation in the big bag. In general, the mixed infra-debris consists of lower quality concrete (e.g. high water-cement ratio) and with a wide range of used types of cements, such as fly ash cements. This stream is therefore further referred to as mixed (waste) ultrafines.
- (2) The second series consists of a waste streams from (railway) sleepers, delivered by Prorail. It consists of a high-strength concrete made with Portland cement as binder. After the pre-crusher, it has been fed into the so-called Smart Liberator, instead of the second crusher. After that, the process is similar to that of the mixed ultrafines. The ultrafines from the sleepers are called sleeper (ultrafines).

At TNO, the sampling codes are MP2017 for the mixed ultrafines and MP2035 for the sleepers. Subcoding 01-13 and 01-08 respectively indicate the bucket number the sample is taken from.

## 3 Characterization tests

## 3.1 Solid density

The solid density was determined at TNO using a Densi 100 gas pycnometer from 3P instruments (see Figure 1).





Figure 1 - Photographs of (left) the Densi 100 gas pycnometer set up and (right) the pycnometer itself with end cap.

The measurement is executed with helium as gas. The pycnometer cup is filled with material and next the helium is added to the cup, until it is completely filled. The solid density then is determined by:

$$\rho_S = \frac{m_S}{(V - V_F)}$$

 $\rho_S$  = solid density [g/cm<sup>3</sup>]

 $m_s = mass of the solid [q]$ 

V<sub>F</sub> = volume of the nitrogen (hollow space) [cm<sup>3</sup>]

V = volume of the pyknometer [cm<sup>3</sup>]

For the mixed ultrafines, one sample for drying is taken from each bucket in order to verify the homogeneity of the sampling. All samples have been dried first at 105 °C until constant weight. For the sleepers, one sample has been taken from bucket 01. The measurements are in five-fold on one sample.

## 3.2 Particle size

A Bettersizer S3 laser diffraction setup from 3P instruments at TNO (see Figure 2) was used to determine the particle size distribution. Samples have been dispersed in isopropanol using the device's internal ultra-sonification procedure to eliminate air bubbles and ensure good dispersion. The samples have not been drying before testing since the dispersion was well.

Laser light is propagated into the solution and the backscattered light is detected by the sensor. Based on the angle of detection, the particle size, in diameter, is determined. Particles up to 3.5 mm can be accurately measured. Besides the particle size, properties with regard to the particle shape such as circularity and aspect ratio, were analysed simultaneously through a dynamic image analysis.



Figure 2 –Bettersizer S3 laser diffraction set-up.

The mixed ultrafines sample has been analysed at Cugla with a Helos laser diffraction sensor combined with Rodos dry dispersion unit and the Vibri vibratory feeder from Sympatech. Sample as received and dried powder have been measured for particle size distribution.

## 3.3 Specific surface area

A Sync 200 surface area and pore size analyser from 3P instruments (see Figure 3) was used at TNO to determine the specific surface area (SBET) of materials. All samples were degassed under vacuum at 350°C for 1 h using a heating mantle. A 3-point SBET measurement was used to derive the specific surface area.



Figure 3 – Photograph of the Sync 200 gas adsorption setup for determining the specific surface area of materials.

### 3.4 Thermal Gravimetric Analysis

Thermal Gravimetric Analysis (TGA) of different samples was performed by measuring the mass loss at different temperatures. Figure 4a shows photographs of the crucibles containing the samples in the oven at TNO. During operation, a nitrogen gas flow is supplied from the back of the oven in order to create a CO<sub>2</sub>-free atmosphere. First, the sample mass was determined at room temperature. Then the temperature was increased to a set value of 105, 400, 500, 600, 700, 800 and 900°C. The time at each temperature until constant mass varied per temperature but was on average around 2 days at 105°C and 4 days at higher temperatures (see **Fout! Verwijzingsbron niet gevonden.**).



Figure 4 - Samples inside the TGA oven

When the samples are at high temperature (>400 °C), they have to cool down first before taking them out the oven and weighing the samples. Therefore, the temperature was decreased to 200 °C for a period of 4-6 hours. When taking the samples from the oven (at 200 °C) to be weighed, the crucibles are immediately covered with a glass plate to avoid exposure to the (moist and CO<sub>2</sub> containing) air.

WUR/WBFR has executed additional TGA on bucket 13 of the mixed ultrafines but in a continuous temperature range (no cooling down again) from 30 to 900 °C.

The moisture content and loss on ignition at 950°C have been determined at Cugla on the mixed ultrafine sample. In order to check whether any moisture gradient was present in the bucket, samples from the top, middle and bottom section of the bucket were analysed, 3 samples per section. The moisture content has been determined by measuring the weight loss following the heating of the samples at 105°C. Subsequently the samples were heated at 950°C for 1h for the determination of the LOI (Loss on ignition). Afterwards the ignited samples were prepared and analysed with X-ray Fluorescence spectrometry (see section XRD/XRF for the specific sample preparation).



Figure 5 Mixed ultrafine sample after LOI at 950°C (Cugla)

### 3.5 Water demand

One of the most crucial component of the mix design of concrete is the water demand of the various components. A fast, subjective way of determining the water demand for the ultrafines is as follows to add water to the (oven dry) materials until a cohesive ball without it falling apart. The water demand is next calculated as the amount of water required to form a cohesive mass relative to the 'as-received material' at TNO.



Figure 6 Fast water demand test: end result

## 3.6 Zetapotential

When solid particles such as the ultrafines are dispersed in water, they will dissolve somewhat, creating a solution that has (in general) a high pH and contains dissolved ions like Na,K,Ca and so on. Due to this dissolution, their surface will be charged, creating a surface potential. Ions of opposite charge present in the surrounding solution will be attracted towards the surface and form layer(s) of (mainly) charge-compensation ions (see Figure 7).

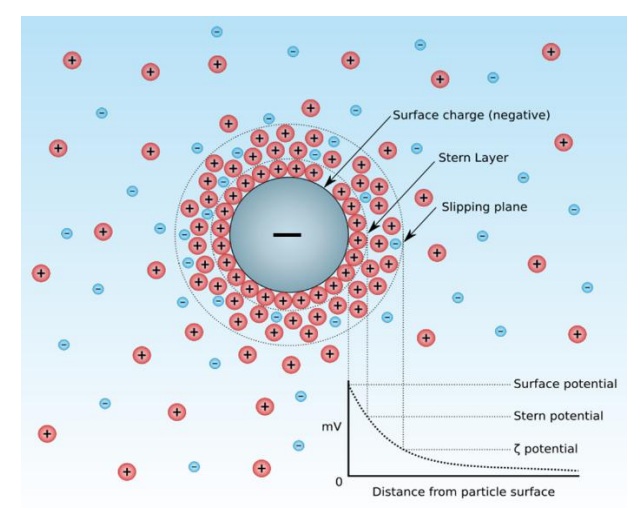


Figure 7 Simplified drawing of the double layer and potential difference as a function of distance from the charged surface of a particle

The zeta potential is a parameter characterizing electrochemical equilibrium at the slipping plane according to Figure 7. It depends on the properties of both the surface and the surrounding liquid. The magnitude of the zeta potential indicates the charge on this plane, and therefore, also the degree of electrostatic repulsion between similarly charged particles. It can also be used to determine the effect of biopolymer additives and their dosage. However, in this characterisation report, only the zeta-potential in demi-water in measured as reference and as characterization, together with the pH and conductivity, in a demi-water solution with a solid / water ratio (on mass) of 1:2. For the measurement, a DT-1202 acoustic spectrometer of 3P instruments was used at TNO. The slurry has been stirred when measuring to ensure a homogenous slurry.

Figure 8 Zeta potential measurement setups showing the set up with four monitoring sensors: zeta potential, conductivity, pH and temperature

### 3.7 XRF/XRD

X-ray diffraction analyses (XRD) have been performed at the TNO laboratorium in Den Haag – Ypenburg. Powder diffraction patterns using a Bruker D8 Advance X-ray diffractometer in Bragg-Brentano geometry with an anti-scatter screen, non-rotating the sample from 8-16° 20 and rotating the sample from 16-66° 20. A

LynxEye detector with opening angle of 2.945°, primary and secondary soller slits of 2.5° and a divergence slit 0.300 mm. Cu-Kα X-rays were generated at 40 kV, 40 mA. Phase identification was performed using Bruker Eva 2.0 software and appropriate databases (ICDD PDF2 2011 and ICSD 2011).

XRD as well as XRF have been determined also by Cugla, on the mixed ultrafines only. For the XRF analysis, fused beads of the mixed ultrafines ignited samples were prepared using an automated fusion instrument Eagon2, and further analysed with Energy Dispersive X-ray Fluorescence (EDXRF) spectrometer Epsilon 4 (Panalytical). XRD analysis have been performed at Cugla on the mixed ultrafines sample, as received (no pre-treatment) and back-loaded. Powder diffraction patterns using a Cubix3 Panalytical X-ray diffractometer in Bragg-Brentano geometry with an anti-scatter screen, non-rotating the sample. Cu-Kα X-rays were generated at 45 kV, 40 mA. Phase identification was performed using HighScore plus software and appropriate databases.

### 3.8 TOC (Total Organic Carbon)

TOC analysis, as used in the present analysis, is a measure of the dissolved organic carbon in solution. This analysis was performed by Cugla in order to determine whether organic carbon will be released from the mixed ultrafines into solution when in contact with water. Organic carbon could possibly delay cement hydration.

Mixed ultrafines and tap water (water/solid=0.5 m/m) were mixed for 3 minutes in an hobart mixer, stand I. The paste was then centrifuged 10 minutes 4000rpm in order to separate the solid from the pore solution. The supernatant was extracted and diluted in demineralized water for TOC analysis. A Lotix TOC combustion analyser (Teledyn Tekmar) was used which utilises a 680°C combustion catalytic oxidation followed by non-dispersive infrared detection to quantify the TOC.

### 3.9 Hardening of the pure materials

In order to investigate the hardening of the ultrafines without any additions, pastes have been made at TNO by mixing the mixed and sleeper ultrafines with water in a (1:1) ratio on weight. Next, small vials have been filled and placed in a isothermal calorimetry equipment (see Figure 9, Figure 10). During more than 60 hours, the heat is recorded that is generated at a constant temperature of 25 °C. After testing, the lid of the vials is removed and the hardening is tested by means of Vicat needle method (see Figure 9). In this test, a needle is place on the surface of the binder paste after which the penetration depth is recorded. If the paste is not hardenend, the needle will drop to the bottom under the gravity force. If the paste on the other hand is hard, it will remain on the paste surface.



Figure 9 Vicat (left) and microcalorimeter (right)



Figure 10 Vials for the microcalorimetry test

Mortar was made with the mixed ultrafines and water according to the EN 196-1 by Cugla and during hardening monitored by means of Ultrsonic Pulse Velocity (UPV IP-8 Ultra-test GmbH), in which the development of the elasticity (dynamic Young's modulus) of the mortar can be monitored. In addition, mortar prism 40x40x160mm have been cast as well to test for compressive strength.

## 4 Characteristics of the ultrafines

## 4.1 Solid density

The solid density of the mixed ultrafines and the sleeper ultrafines are given in Table 1. Since each sample is measured five times, and the standard deviations of the measurements on the same sample are extremely low (< 0.01 %), these values are further presented without standard deviations. The density of the mixed ultrafines have been determined 13 times. From each of the 13 buckets, one sample has been taken randomly. The largest individual measurement deviated 3.3 % from the average, the standard deviation of the 13 samples combined is less than 2.5 %. This indicates that the sampling of the mixed ultrafines from the big bag has been good.

Table 1 Solid density of the ultrafines

ultrafines	density (kg/m3)			
	average	standard deviation		
mixed	2.323	0.060		
sleepers	2.409			

The density of the sleepers is slightly higher than for the mixed ultrafines but still less than for e.g. unreacted cement (density ca. 3.1) or sand /gravel (density ca. 2.65). It is, however, more than reacted cement alone (density 2.2 or less depending on the original water to cement ratio and used cement). In addition, in the mixed ultrafines also other materials may be present such as (unreacted) fly ash.

### 4.2 Particle size distribution

The particle distributions of the ultrafines as determined by wet laser method at TNO are shown Figure 11. For comparison, also the particle size distribution of GGBS or slag is shown. Some characteristics of the particle size distribution are further given in Figure 11. The particle size distribution of the mixed ultrafines by dry laser method at Cugla's is given in Figure 12.

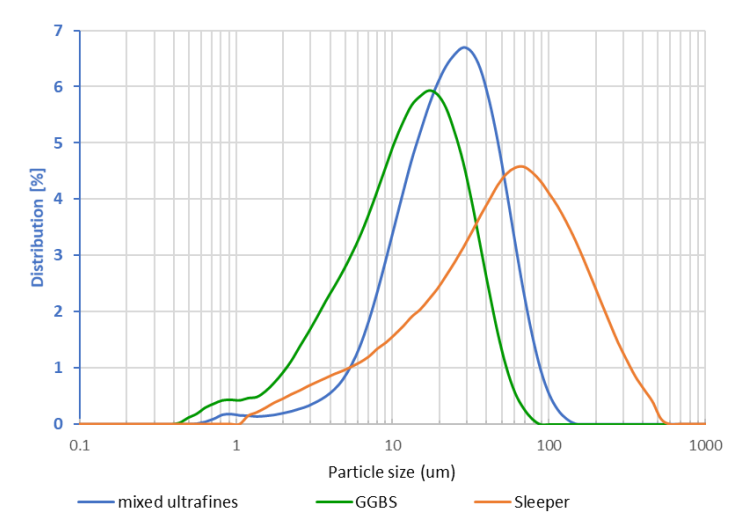


Figure 11 Particle size distribution for a single sample (wet method)

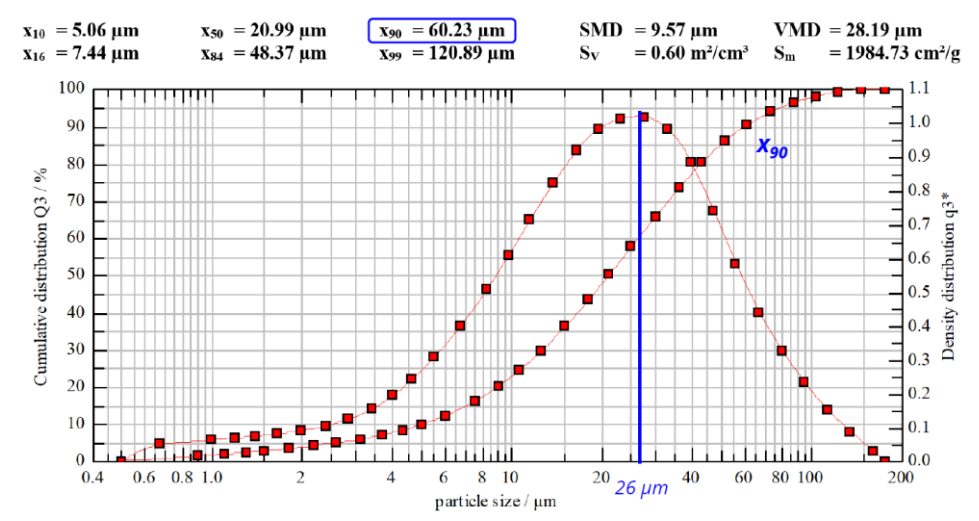


Figure 12 Particle size distribution for a single sample (dry method)

In Table 2, the particle sizes are given at 10 %, 50 % and 90 % of the particles. Data are shown for both wet (TNO) and dry methode (Cugla , Urban Mine). In addition, the data of TNO are averages of 13 samples for the mixed ultrafines since one sample from each bucket has been tested while for the sleeper ultrafines, it is the average of 10 samples, also one from each bucket. It may be notices that the standard deviation is 5-6 % for d50 and d10 but ca 9 % of d90.

Table 2 Particles sizes at 10, 50 and 90 % of the particles results of TNO and Cugla for the mixed ultrafines and TNO and Urban Mine (UM) for the sleeper. Cugla and Urban mine used a dry dispersion laser method, TNO a wet laser method.

	MIXED ULTRAFINES	SLEEPER
	(wet TNO/dry Cugla)	(wet / dry UM)
d90 (μm)	52.5 (4.6) / 60.2	173.8 (15.4) / 177.1
d50 (μm)	22.6 (1.2) / 20.1	47.2 (2.9) /51.2
d10 (μm)	7.7 (0.3) / 5.1	6.7 (0.4) / 2.9

### 4.3 Specific surface area and porosity

The specific surface area and (internal) porosity have been determined at TNO on 5 samples taken randomly from 5 different buckets for the mixed ultafines; for the sleepers only a single specimen has been tested. For comparison, also the specific surface of slag is given. Since this is a nonporous material, it does not have a pore volume. It can be seen that the sleeper ultrafines have a specific surface that is somewhat more than twice as large that than of the slag which indicates, together with the much coarser particle size distribution that its (N2-reachable) surface is much more tortuous than for the slag. At the same time, it is also porous, which (internal) surface is also part of the specific surface area, although it is only 0.002 ml/g dry solid material. The mixed ultrafines show a 4 times as large porosity and a finer particles distribution compared to the sleeper ultrafines, both characteristic contribute to the much higher specific surface area. Both have a reported average pore diameter which is at the detection level of the method.

Table 3 Specific surface (SBET) surface area of the ultrafines and pore volume per gram of solid materials

	surface area [m2/g]	Pore volume [ml/g]	Average pore diameter [nm]
mixed	15.2 (1.5)	0.008 (0.001)	1.96 (0.01)
sleeper	3.4	0.002	1.97
slag	1.4	-	-

### 4.4 Moisture content

At TNO, the moisture content has been determined by oven drying the ultrafines from 20 °C to 105 °C. Both the mixed ultrafines and the sleeper ultrafines have been determined on 5 different samples from 1 bucket (number 5 and number 1 respectively). The results are shown in Table 4. At Cugla, 6 samples have similarly oven dried to 105 °C from bucket 6 of the mixed ultrafines. Samples have been taken from 3 layers of the buckets. The results are given in Table 5. At the WFBR, the specimens had to pre-dried to 30 °C before they could be tested in the TGA (see next sections), no separate tests have been run. At TNO, a rerun of the moisture content test have been executed to investigate if the moisture content was indeed very different across the buckets and indeed found a 5 % difference in moisture content between bucket 3 and 5.

Table 4 Moisture content in wt-%, TNO and Cugla: as received start (at 20 °C), standard deviations between brackets

	mixed	sleeper
TNO (105 °C)	B5: 23.3 (0.4)	B1: 7.3 (0.2)
	B3: 18.3 (0.2)	
Cugla (105 °C)	B6: 14.3 (0.3)	-
WUR (30 – 100 °C)	B13-serie 1: 14.9	4.7
(30 -105 °C)	B13-serie 2: 12.5	

% mass loss Av. % mass loss Top-1 14,4% 14,5% Top-2 14,4% Top-3 14,7% Middle -1 14,0% Middle -2 14,0% 14,2% Middle -3 14,5% Bottom -1 13,9% Bottom -2 14,5% 14,2% Bottom -3 14,3%

Table 5 Moisture content of the mixed ultrafines - bucket 6 (results Cugla)

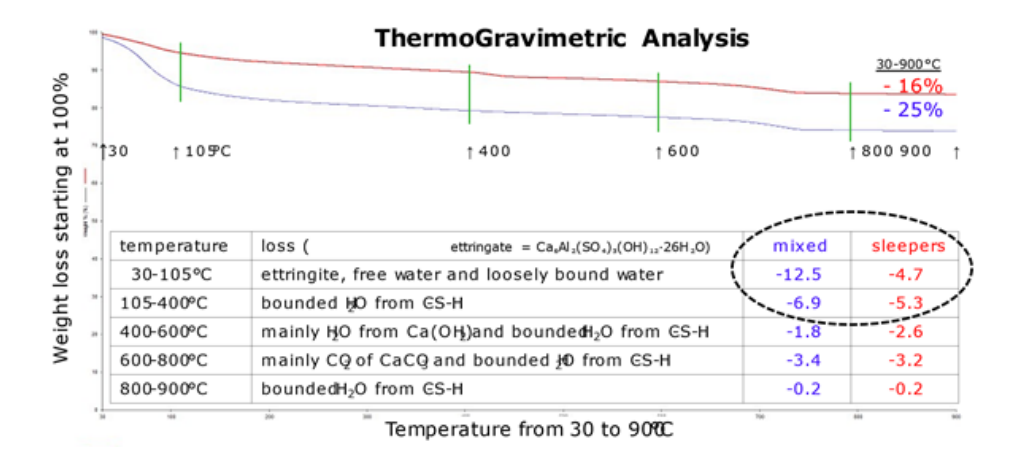
The results indicate that although the moisture content seems to equilibrate quickly enough in the buckets, the moisture content of the mixed ultrafines seem to differ considerably per bucket, despite the fact that they have been sampled randomly and at the same location and time.

### 4.5 TGA and loss on Ignition

In Table 6, the loss of ignition (LOI) is given. Only Cugla has heated the specimens to the prescribed 950  $^{\circ}$ C, while TNO and WUR have heated the specimens up to 900  $^{\circ}$ C. The LOIs of the mixed ultrafines and sleepers of WUR and TNO match well, but the distribution of the moisture content within the 105 – 900  $^{\circ}$ C can be seen to differ (comparing Figure 13 and Figure 14, Table 7).

Table 6 LOI in wt-% (TNO/WUR only up to 900 oC instead of 950 oC)

	mixed	sleeper
TNO (900 °C)	12.0 (0.1)	11.2 (0.3)
Cugla (950 °C)	27.8	-
WUR (900 °C)	12.3	11.3



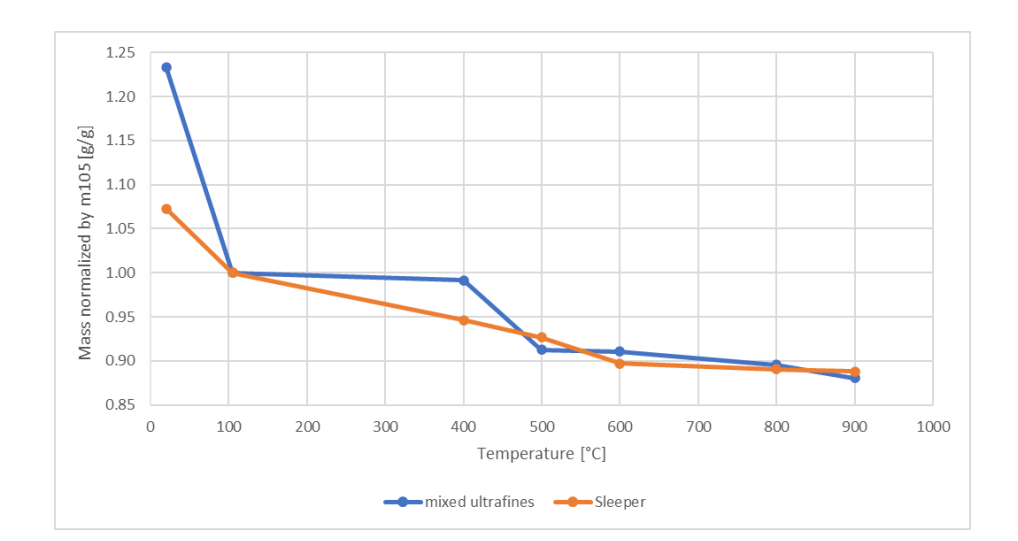


Figure 13 TGA-profile of mixed and sleeper ultrafines measured at WUR

Figure 14 TGA-profile of mixed and sleeper ultrafines measured at TNO

Table 7 Mass loss in wt-% relative to the mass at 105 °C and a possible interpretation of the mass losses (assuming no organics are present)

		105-400	400-600	600-800	800-900	LOI
mixed	TNO	0.9	8.1	1.5	1.5	12.0
ultrafines	WUR	6.9	1.8	3.4	0.2	12.3
sleepers	TNO	5.4	4.9	0.7	0.3	11.2
	WUR	5.3	2.6	3.2	0.2	11.3
Origin mass loss		Progressive loss of water from CSH				
			Water	CO <sub>2</sub>		
			from	from		
			Ca(OH) <sub>2</sub>	CaCO₃		

Comparing the results, it thus seems that there is quite some different in moisture contents over the buckets (Section 4.5), despite the fact that the buckets have been samples at the same time and by random scooping simultaneously in all buckets. Furthermore, it seems that when adding the total mass loss is quite constant but the mass losses in specific temperature ranges can vary considerably. Different testing methods (with/without fan, under  $N_2$ ) and slightly different start and end temperatures may therefore account for some of the difference.

### 4.6 Water demand in the quick consistency test

The results of the quick, subjective, water demand tests are shown in Figure 15 and Table 8. It can be seen that at similar consistency, the sleeper ultrafines require less water than the slag. However, when expressed as water demand, the water demand of the mixed ultrafines proves to be more than twice as low, as a consequence of its high specific surface area.





Figure 15 Determining the water demand on the basis of a quick, global consistency method: left mixed ultrafines and right sleeper ultrafines.

	Water demand (g/g as received material)	Moisture content (g/g dry material)	Total water demand (g/g dry material)	surface area (m2/g)	water demand (g/m2)
mixed	0.40	0.23	0.77	15.2	0.05
sleepers	0.30	0.07	0.40	3.4	0.12

0.40

1.4

0.29

0.00

Table 8 Water demand of the ultrafines, slag is shown for comparison

### 4.7 Characteristics of the ultrafines in water

slag

0.40

In Table 9, the specifics of the ultrafines in demi water are given. It can be seen that the mixed ultrafines give rise to a high (equilibrium) pH of 12.6 (mixed) and 12.9 (sleepers). For comparison: slag has a pH of only 9.9, which is considering the log-scale of the pH, considerable. This difference is in part reflected in the high conductivity of the ultrafines, indicating as well that upon mixing, part of the material dissolved immediately. In general the fastest dissolving elements from the solids are the most mobile ones: the alkalis (Na, K) and chloride, sulfates and hydroxides (the latter giving the high pH).

The zetapotential of the mixed ultrafines is lower than for the sleepers, indicating that the average charge at the zeta potential plane around the mixed ultrafines is lower. This is also reflected in the lower water demand per m², which indicates the amount of water required to have a certain loss of friction between the particles, to reach a fixed consistency (see Table 9). There is, however, no one-to-one relationship between these two parameters. Amongst others, also the ionic strength of the solution helps to reduce the water low concentration of counter-charging ions in the solution is in part the reason why the slag has a high water demand per m².

	pН	Conductivity	Zetapotential	water demand
	(-)	(S/m)	(mV)	(g/m2)
mixed	12.6	0.35	0.6	0.05
sleepers	12.9	0.53	1.7	0.12
slag	9.9	0.02	1.4	0.29

Table 9 Specifics of the ultrafines and slag in water and water demand of the material from the quick consistency test

#### 4.8 XRF

The results of the XRF analysis of Cugla on the mixed ultrafines are shown in Table 10. Sample preparation for XRF is described in section 3.7. Fused beads have been prepared on ignited samples, water and carbonates have been already eliminated.

Table 10 XRF ana	ysis of the mixed ultra	afines (Cugla)

			wt.%		Ì
Oxide					
Oxide	sample 1	sample 2	sample 3	average	Sdt
Na <sub>2</sub> O	0,400	0,326	0,325	0,350	0,043
MgO	2,018	2,075	2,006	2,033	0,037
Al <sub>2</sub> O <sub>3</sub>	7,768	7,824	7,785	7,792	0,029
SiO <sub>2</sub>	56,875	56,389	56,946	56,737	0,303
SO₃	1,863	1,905	1,866	1,878	0,023
K <sub>2</sub> O	1,025	1,017	1,060	1,034	0,023
CaO	27,329	27,772	27,284	27,461	0,270
MnO <sub>3</sub>	0,135	0,140	0,133	0,136	0,003
Fe <sub>2</sub> O <sub>3</sub>	2,587	2,553	2,595	2,578	0,023
tot	100	100	100	100	

Both silicate and calcium oxide are present in high amount, which are the major components of the aggregates (quartz for river sand and gravel, and calcium in calcium carbonate aggregates like lime stone) as well as the cement.

Based on the cement composition of ENCI in the 1980-1990's (ENCI product bladen, ENCI, Den Bosch), the composition of Portland fly ash cement CEM II/B-V 32.5 R contains 25 % SiO<sub>2</sub>, pure Portland cement and blast furnace slag cement ca. 30 % and composite cement CEM II/B-M 20-30 %. At the same time, these cements have a CaO content between 21 to 30 % for the blended cement and 64 % for CEM I and a SO<sub>3</sub> contents of the cement (between 2.8 to 3.3 %). Combining these numbers indicate that the ultrafines contain possibly only 50 % old cement paste and 50 % milled sand and gravel, assuming all Ca is due to the cement and not due to carbonate-containing aggregates and that blended cements have been used. Under these provisions, the 50/50 % estimate is thus a (coarse) minimum estimate.

### 4.9 XRD

XRD-analyses have been executed at TNO for both ultrafine materials (Figure 16, Figure 17) and Cugla for the mixed ultrafines (Figure 18). In addition, Urban Mine made also an analysis for the sleeper ultrafines (Table 11). The XRD analysis at

TNO show that the silicate may be present as quartz, or a few other minerals. Urban Mine (Table 11) also reported the presence of larnite, being likely an unreacted cement clinker. A part of the silica will also be present in the amorphous CSH (reacted cement gel), which the XRD cannot analyse (only the presence of amorphous phases can be detected). Furthermore, the minerals albite (likely from the aggregates), calcite (either as aggregate, filler or carbonated hardened cement paste / calcium hydroxide), ettringite (usually formed at the cement hydration, sometimes formed in a later stadium). Only the sleeper ultrafines contain portlandite (Ca(OH)<sub>2</sub>)). Urban Mine detected in the sleeper ultrafines dolomite (either as aggregate or filler) and AFm (a cement reaction product formed during hydration of the cement).

Two unexpected phases were detected both by TNO and Urban Mine. The first one was clinochlorite, a member of the chloride group of minerals (identified as chlorite by Urban Mine) and by both TNO and Urban Mine expected to be part of the granulate, if some natural stone has been present in the recycled concrete. The second phase might be bedeillite ("2:1 phyllosilicates") and might also be part of the aggregates that were used in the primary concrete (or perhaps contamination?).

Table 11 XRD minerals in the sleeper ultrafines determined by Urban Mine (Email A. Alberda, dd. 21-12-2022):

- silicates	
0	quartz SiO <sub>2</sub>
0	K-feldspar KAlSi <sub>3</sub> O <sub>8</sub>
0	Plagioclase (Na,Ca)(Si,Al) <sub>4</sub> O <sub>8</sub>
0	Beta C2S* (Larnite) Ca <sub>2</sub> SiO <sub>4</sub>
0	2:1 phyllosilicates (K,H <sub>3</sub> O)(Al,Mg,Fe) <sub>2</sub> (Si,Al) <sub>4</sub> O <sub>10</sub> [(OH) <sub>2</sub> ,(H <sub>2</sub> O)]
0	Chloriet (Mg,Fe) <sub>5</sub> Al(Si <sub>3</sub> Al)O <sub>10</sub> (OH) <sub>8</sub>
<ul> <li>carbona</li> </ul>	tes
0	Calcite CaCO <sub>3</sub>
0	Dolomite/Ankerite Ca(Fe <sup>2+</sup> ,Mg,Mn)(CO <sub>3</sub> ) <sub>2</sub>
0	AFm*** Ca2Al(OH)6[Cl1-x(OH)x]•3(H2O)
<ul> <li>sulfates</li> </ul>	
0	Ettringite/AFt** Ca6Al2(SO4)3(OH)12•26(H2O)
- oxides/h	ydroxides
0	Portlandite Ca(OH)2
- Others /	amorph

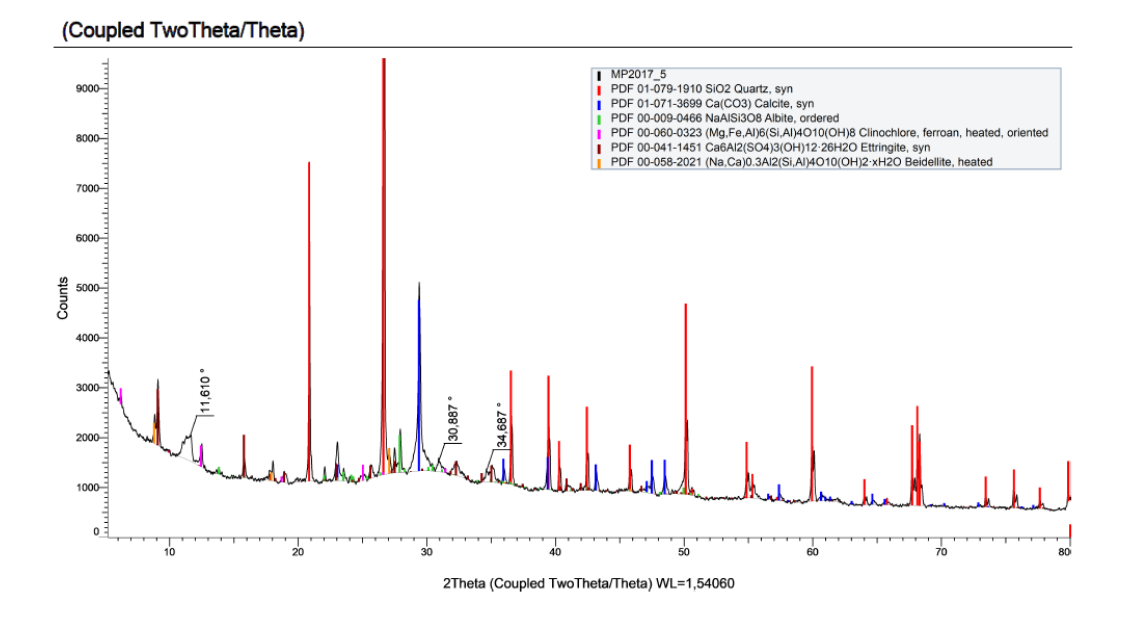


Figure 16 XRD diffractogram for the mixed ultrafines measured at TNO

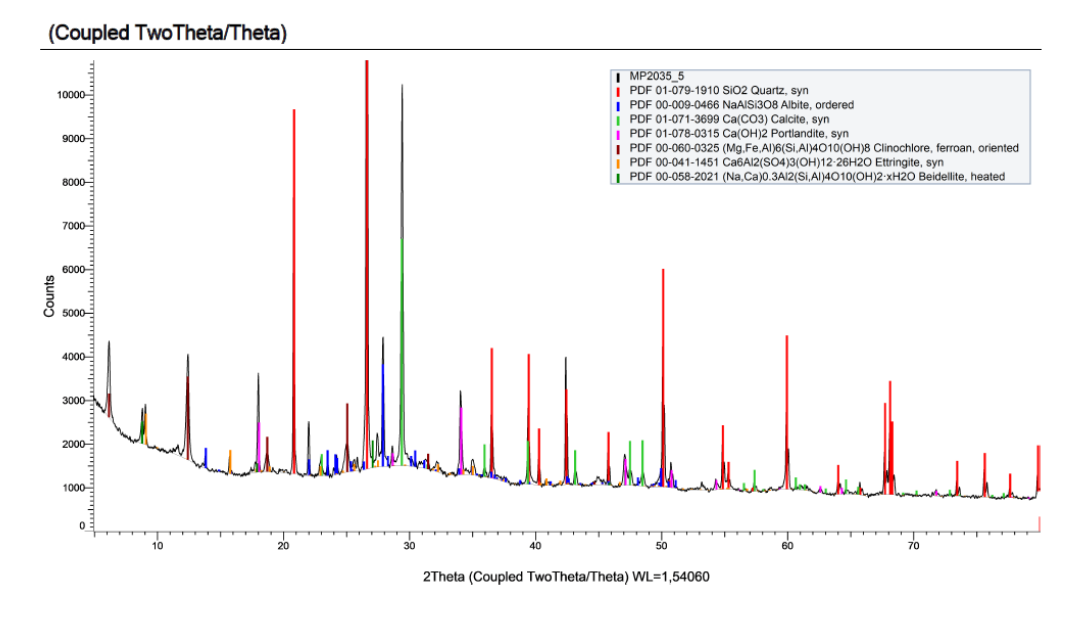


Figure 17 XRD diffractogram for the mixed ultrafines measured at TNO

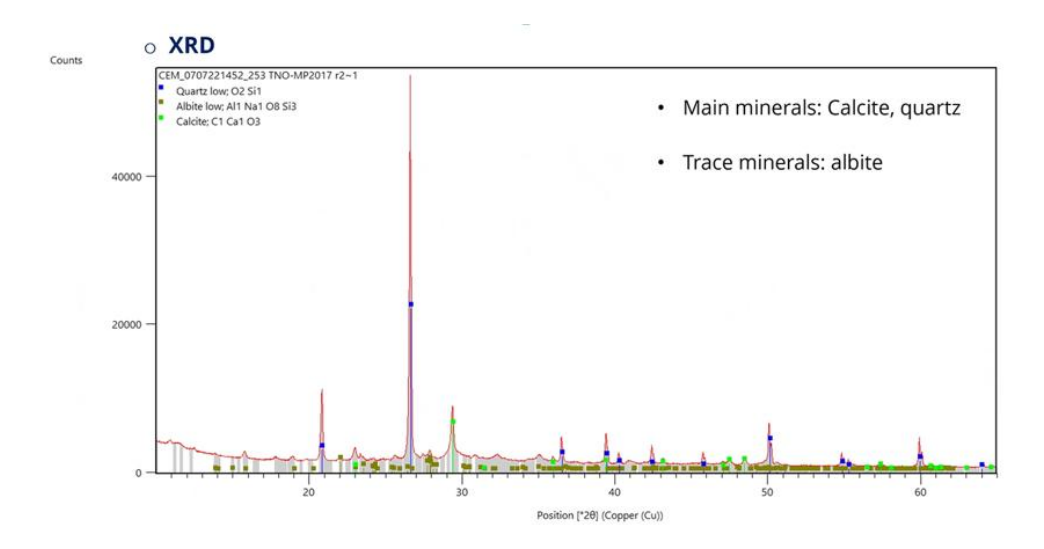


Figure 18 XRD diffractogram for the mixed ultrafines measured at Cugla

### 4.10 TOC

The total organic carbon, as measured by means of the total soluble carbon, was for the mixed ultrafines found to be 224 ppm. As comparison, the TOC content of CEM I paste (w/c = 0.5) has been measured in the range 200-540 ppm and paste of CEM III/A (ca. 50 % Portland cement clinker and 50 % slag): around 210 ppm. Paste consisting of slag and water exhibited a TOC content of 5 ppm. The soluble TOC measured in cement paste mainly comes from chemical grinding aids used during the grinding of cement. The TOC content released in solution from paste of mixed ultrafines is in the same range of the TOC of cement paste. However, no conclusion can be drawn on the nature of the organic carbon.

Although the TOC-values are in the same range, it seems unlikely to find the same and as much grinding aid from cement in the recycled concrete (after hydration and years later). Possibly, therefore, the similarity in TOC's is coincident and the nature/origin of this organic carbon is different.

## 4.11 Hardening of the pure materials

In Figure 19, the heat development of the mixed ultrafines paste is shown, for the 'pure' ultrafines but also with a set regulator. Despite the fact that with set regulator, the mixes produce more heat (indicative of the occurrence of exothermic chemical reactions), after more than 60 hours curing at 25 °C, the mixes had not hardened. Also in the UPV test and compressive strength test on mortar, the mixed ultrafines showed no reactivity nor developed any strength (Figure 20,

Figure 21). Likewise, the sleeper ultrafines did not harden when mixed with water alone. Adding set-regular improved the hardening somewhat. However, after one week even the specimens still had no strength.

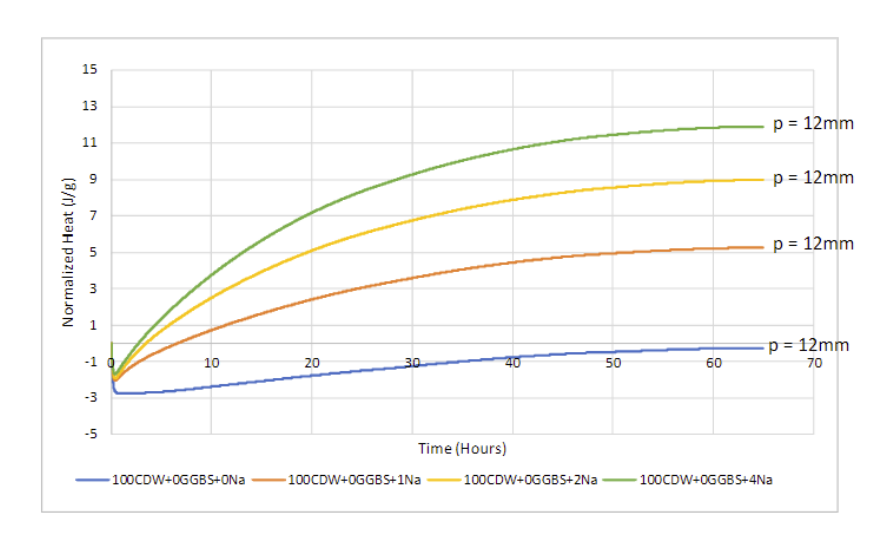


Figure 19 Heat development of mixed ultrafines (CDW) with water and set regulator (Na) with various, p=12 means penetration in the Vicat test = 12 mm)

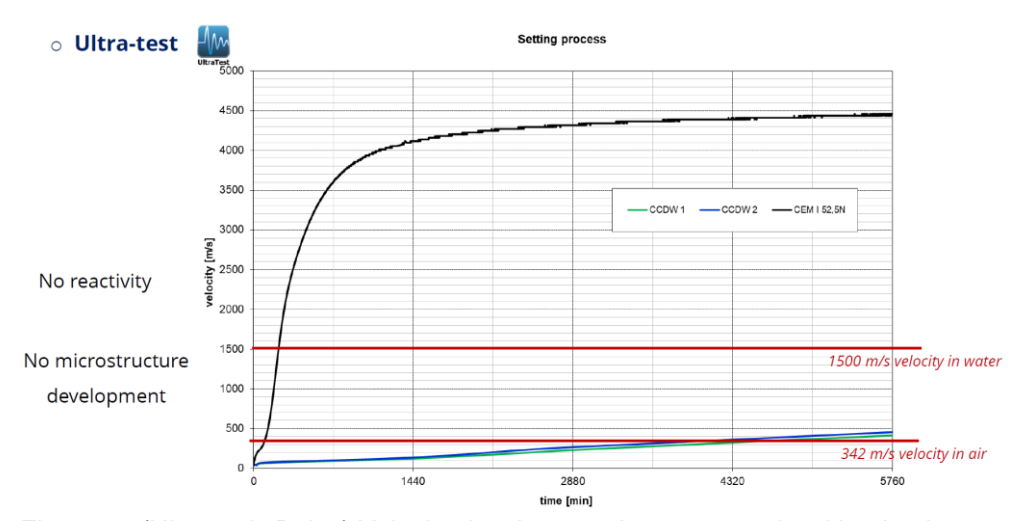


Figure 20 (Ultrasonic Pulse) Velocity development in mortar made with mixed ultrafines (CDW 1 and CDW2), as compared to CEM I 52.5 N

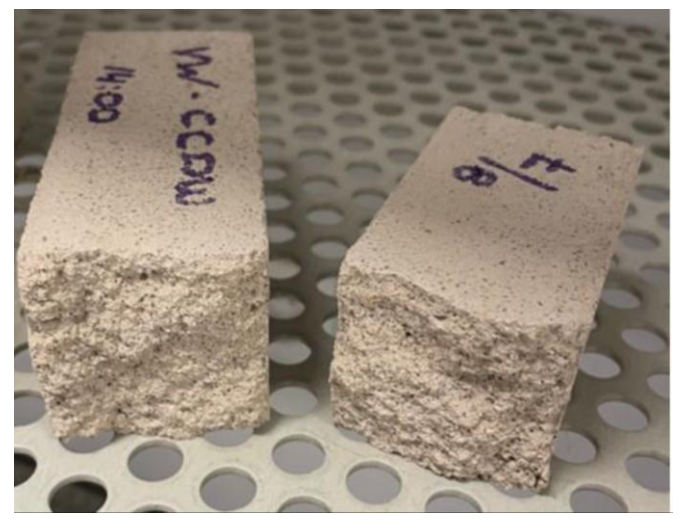


Figure 21 Mortar bar made with the mixed ultrafines: the bar has no strength and can be broken by hand.

## 5 Discussion and conclusions

In this report, two streams of ultrafine recycled concrete waste streams have been characterized. Both were produced by Urban Mine. The first ultrafines came from mixed 'infra-debris', consisting of concrete goods like (sidewalk) tiles and curbs. The second series consists of a waste streams from (railway) sleepers, delivered by Prorail to Urban Mine.

### 5.1 Composition

XRD analysis showed that both streams consisted of quartz, calcium carbonate, albite and ettringite as mineral phases, with portlandite also found in the sleeper ultrafines. Two other minerals found were likely present in the aggregates (or contamination ?). The quartz is likely from milled sand and gravel, while the calcium carbonated may come from either carbonated cement products (portlandite or CSH) or aggregates or fillers. Ettringite is most likely a cement hydrate products. Most of the cement hydrates, however, will be amorphous, and cannot be analysed in the XRD. Furthermore, it can be deducted from the presence of the portlandite that at least not all cement paste of the sleepers is carbonated. For the mixed ultrafines, the composition may have been too low in calcium content to have led to formation of portlandite, hence no indication of carbonation of the cement paste can be made. XRF analysis of the mixed ultrafines, combined with the knowledge of the most commonly used cements in the Netherlands, makes it likely that show that the mixed ultrafines contain possibly only 50 % old cement paste and 50 % milled sand and gravel, assuming all Ca is due to the cement and not due to carbonatecontaining aggregates and that blended cements have been used. Considering the presence of dolomite, this is an lower limit of the old cement paste. No XRFanalysis of the sleeper ultrafines have been available.. Since these sleepers have been recycled in a different process, their ratio of sand / old cement paste may be different. Both ultrafines are in addition basic: when mixed with water they both lead to a solution that has a pH of 12 6 (mix) and 12.9 (sleepers), indicative of an equilibrium with the calcium phases (Ca(OH)2 or calcium-poor CSH phases) and some alkalis which lead to reasonably high conductivities (0.35 S/m and 0.53 S/m for the mixed and sleeper ultrafines respectively). The pH is however well below that of uncarbonated CEM I which, depending on the amount of alkalis has a pH of 13.2 to 13.6. In terms of LOI (up to 900 °C)both ultrafines were recorded to have 11-12 % weight loss compared to the weight at 105 °C. This weight loss can be due to organic carbon, chemically bound CO2 and water. Only Cugla measured a very high LOI for the mixed sleepers (27%), the accompany lower weight loss up to 105 °C makes it possible that quite some part of this weight loss will be lost at comparatively low temperatures (higher than but close to 105 °C).

## 5.2 Physical characteristics and water demand

Density, particle size distribution and specific surface area have been measured, in addition to an estimate on the internal pore volume and pore sizes of the ultrafines. The characteristics are summarized in Table 12. The major difference between the two ultrafines is the size: the sleeper ultrafines are coarser. At the same time, even though the mixed fines are finer in size, they have a considerable higher amount of

internal pres., As a consequence the surface area of the mixed fines (internal and external!) is much higher. The pore size in the ultrafines was estimated for both materials to be 2 nm, which is at the precision of the equipment and thus needs to be taken as indicative.

Table 12 Summary of the physical characters of the ultrafines

	Density				water
	$(kg/m^3)$		surface area	Pore volume	demand
		D50 (nm)	$(m^2/g)$	[ml/g]	$(g/m^2)$
mixed	2.323	22.6	15.2 (1.5)	0.008 (0.001)	0.05
sleeper	2.409	47.2	3.4	0.002	0.12

### 5.3 Reactivity

When mixed with water, both ultrafines dissolve to some extent, giving rise to a high pH and conductivity. The zetapotential of the mixed ultrafines is lower than for the sleepers, indicating that the average charge at the zeta potential plane around the mixed ultrafines is lower. This is also reflected in the lower water demand per m², which indicates the amount of water required to have a certain loss of friction between the particles, to reach a fixed consistency (see Table 9). There is however no one-to-one relationship between these two parameters. Amongst others, also the ionic strength of the solution helps to reduce the water demand up to a certain level, after which is becomes counter-effective.

The dissolution experiments show that part of the ultrafines dissolve until reaching a (semi-) equilibrium. After that, however, no discernible reaction has been observed in the micro-calorimeter followed by Vicat (on paste) or UPV and strength measurement (on mortar). Set regulator help to improve the reaction (rate), resulting in better Vicat needle penetrations results, but the reaction is not enough to obtain strength within 7 days. Other additives thus are required to help the ultrafines to react better.

# 6 Signature

Delft, 22 March 2023

TNO

Dr. J.H.M. Visser Author

T.J.A. Dijkmans MSc Project Manager

Ir.ing. M. Steins Research manager Building Materials&Structures